Nat. Hazards Earth Syst. Sci. Discuss., doi:10.5194/nhess-2016-11, 2016
Manuscript under review for journal Nat. Hazards Earth Syst. Sci.
Published: 26 January 2016

Natural Hazards and Earth System Sciences
Open Access
Discussions

First GPS TEC maps of ionospheric disturbances induced by reflected tsunami waves: The Tohoku case study

L. Tang[1, 2], Y. Zhao[1] and J. An[3]

[1] Key Laboratory of Earthquake Geodesy, Institute of Seismology, China Earthquake Administration, Wuhan 430071, China

[2] School of Geodesy and Geomatics, Wuhan University, Wuhan 430079, China

[3] Chinese Antarctic Center of Surveying and Mapping, Wuhan University, Wuhan 430079, China

Correspondence to: L. Tang (ltang@whu.edu.cn)

Abstract

The straight tsunami waves from epicenter can be reflected when they reach to coasts or underwater obstacles. In this study, we present the first ionospheric maps of reflected tsunami signature caused by the great 11 March 2011 Tohoku earthquake using the dense GPS network GEONET in Japan. We observed tsunami-like travelling ionospheric disturbances (TIDs) with similar propagation characteristics in terms of waveform, horizontal velocity, direction, period and arrival time compared to the reflected tsunami at the sea-level, indicating the TIDs are induced by the reflected tsunami. The results confirm the atmospheric internal gravity waves (IGWs) produced by reflected tsunami can also propagate upward to the atmosphere and interact with the plasma at the ionospheric height.

Keywords: GPS; total electron content; traveling ionospheric disturbances; reflected tsunami

1 Introduction

A tsunami propagating in an open ocean can produce atmospheric internal gravity waves (IGWs) and they are significantly amplified when propagate upward to the ionosphere (Hines, 1972; Peltier and Hines, 1976). The IGWs interact with the ionospheric plasma and might generate the signatures that can be detectable by ionospheric sounding.

The detection of ionospheric signature caused by a tsunami began at 2005 on the case of the 2001 Chile earthquake, which was performed by using the ionospheric imaging derived from very dense Japanese GPS Earth Observation Network (GEONET) (Artru et al., 2005). After that many scholars also observed tsunami-driven TIDs in measurements of ionospheric total electron content (TEC) derived from ground-based GPS stations (DasGupta et al., 2006; Rolland et al., 2010; Liu et al., 2011; Galvan et al., 2011; Occhipinti et al., 2013; Tang et al., 2015; Zhang and Tang, 2015) and satellite-based altimeters (Occhipinti et al., 2006), Doppler sounders (Liu et al., 2006) and airglow images (Makela et al., 2011; Occhipinti et al., 2011). Furthermore, the numerical modeling can also show evidences that ionosphere is a sensitive medium to tsunami propagation (Occhipinti et al., 2006; Mai and Kiang, 2009; Hickey et al., 2009).

Previous studies focused on the ionospheric signature induced by straight tsunami waves. For a big size tsunami, its waves propagate to the coasts or underwater obstacles, the reflected waves might be generated. A reflected tsunami waves were observed at the sea-level for the May 2006 Tonga tsunami (Tang et al., 2008). Rozhnoi et al. (2014) observed a signature in low ionosphere, which possible was generated by the reflected tsunami, following the 2010 Chile earthquake with the VLF signals. However, the VLF signals can only provide us a single time-series with the observation time and period of the ionospheric disturbances; other significant propagation characteristics such as horizontal velocity and direction are not presented. Whether the IGWs induced by the reflected tsunami waves can propagate to ionosphere is still unclear.

In this study, we will apply the two-dimensional TEC maps derived from a dense GPS network (GEONET) to detect the possible reflected tsunami signature in ionosphere after the 2011 Tohoku earthquake. The TEC maps can image propagation of TIDs over lager areas, which are very suitable for the ionospheric monitoring.

2 Method

Due to the high spatial and temporal resolution, GPS ionospheric monitoring has been a powerful tool for remote sensing of the ionosphere. The parameter using in GPS ionospheric monitoring is ionospheric TEC (sTEC), the integrated electron density along the entire line-

Nat. Hazards Earth Syst. Sci. Discuss., doi:10.5194/nhess-2016-11, 2016
Manuscript under review for journal Nat. Hazards Earth Syst. Sci.
Published: 26 January 2016

of-sight (LOS) between receiver and satellite. The sTEC can be calculated from the geometry-free combination of GPS dual-frequency carrier phases for each satellite-receiver pair, namely

$$s_T = \frac{1}{40.3}\frac{f_1^2 f_2^2}{f_1^2 - f_2^2}\left(L_1 - L_2 + const + \varepsilon\right) \quad (1)$$

where s_T is the sTEC with unit of TECU (1 TECU=10^{16}/m^2); f_1 (1575.42 MHz) and f_2 (1227.60 MHz) are the carrier phase frequencies, respectively, L_1 and L_2 are carrier phase observations with unit of meter, respectively; $const$ is the unknown constant bias, including the ambiguity and instrument bias; ε is the measurement noise. A single-layer model with height of 350 km is used to obtain the vertical TEC (vTEC) $v_T(t)$ and position of ionospheric pierce point (IPP).

Although Eq. (1) cannot acquire the absolute value of TEC at a particular time due to the unknown bias, it can capture the TEC variation over time with high precision, which is important for TIDs detection. In this paper, we employ a numerical difference method to eliminate the diurnal variation and the bias in TEC and extract the vTEC variation series (Hernández-Pajares et al., 2006; Tang and Zhang, 2014)

$$d(t) = v_T(t) - 0.5(v_T(t-\tau) + v_T(t+\tau)) \quad (2)$$

where $d(t)$ is the vTEC variation; t is the observation epoch; τ is the time step for difference. The time step is set to 300 s, which is suitable for the TIDs detection induced by the IGWs. The numerical difference method is very simple and beneficial to process large number of data.

The number of the ground-based stations in GEONET is about 1200 and data sampling rate is 30 s. The average distance between GEONET stations is about 25 km, providing us a good opportunity to monitor the ionosphere with high resolution. After processing the data from all GPS stations, we can plot the vTEC variation values with different IPPs at specific epoch in a two-dimensional map. The two-dimensional maps of vTEC variation will be used to detect the tsunami signature in ionosphere.

Nat. Hazards Earth Syst. Sci. Discuss., doi:10.5194/nhess-2016-11, 2016
Manuscript under review for journal Nat. Hazards Earth Syst. Sci.
Published: 26 January 2016

3 Results and Analysis

3.1 Reflected tsunami signatures at sea-level

According to U.S. Geological Survey, the Tohoku (Japan) earthquake (Mw=9) with epicenter located at 38.297°N, 142.373°E occurred at 05:46 UT on 11 March 2011 and then triggered powerful tsunami. Figure 1 indicates the locations of epicenter and Deep-ocean Assessments and Reporting of Tsunami (DART) bottom pressure stations operated by the National Data Buoy Center (NDBC) of U.S. National Oceanic and Atmospheric Administration (NOAA). As showing in Figure 1, when straight tsunami waves from epicenter propagate to the Emperor seamounts (average depth ~2000 km), the reflected waves might be generated due to the powerful energy.

To confirm the existence of reflected tsunami waves, Figure 2 presents the sea-level measurements recorded by the DART 21401 and DART 21419. The DART 21401 that near the epicenter first observes the straight tsunami at 06:46 UT and then the waves propagates to the DART 21419 at 07:09 UT. However, the DART 21419 and DART 21401 observes another augmented signal at 09:28 UT and at 09:52 UT, suggesting there are tsunami waves propagated along the opposite direction of the straight tsunami waves. Furthermore, the amplitude of the waves recorded in DART 21419 (0.139 m) is slightly larger than that in DART 21401 (0.111 m), which can serve as further evidence that the waves propagated from DART 21419 to DART 21401. As shown in Figure 2, the spectral analysis for the time-series of the tsunami signals indicate they have similar center frequency of ~0.40 mHz. Another significant signal (~0.66 mHz) in time-series of DART 21401 is the frequency of straight tsunami (Makela et al., 2011; Occhipinti et al., 2011).

In addition, the model of sea-level variation due to tsunami waves can further support the reflected tsunami waves. The NOAA's Method of Splitting Tsunami (MOST) model (see the animation for Tohoku tsunami: ftp://ftp.pmel.noaa.gov/tsunami/honshu/) can offer the propagation characteristics of the reflected tsunami at the sea-level. According to the MOST model, the straight tsunami waves reach the Emperor seamounts at about 3 h after the earthquake. Then, the tsunami waves are divided into two parts: one part continued to propagate ahead, another part along the opposite direction. The opposite tsunami waves pass the DART 21419 and DART 21401 successively, and reach the epicenter at about 6 h after the earthquake.

In short, the observation results by DARTs and the MOST model results demonstrate that there were reflected tsunami waves at the sea-level with frequency about 0.40 mHz.

3.2 Reflected tsunami signatures in ionosphere

The ionospheric disturbances induced by origins from epicenter such as Rayleigh waves, acoustic-gravity waves and gravity waves (tsunami waves) were observed by several scholars after the 11 March 2011 Tohoku earthquake (Liu et al., 2011; Rolland et al., 2011; Tsugawa et al., 2011; Occhipinti et al., 2013; Occhipinti, 2015). Here, we focus on possible reflected tsunami signature in ionosphere induced by this event.

Figure 3 presents the two-dimensional maps of vTEC variations derived from GPS observations in GEONET on 11 March 2011 at studied times. As shown in the upper left panel, the ionospheric disturbances induced by origins from epicenter are basically invisible at about 08:30 UT. However, TIDs (indicated by the blue arrow) began to appear again at about 11:50 UT. As shown in Figure 3, the TIDs propagated along the southwest that is accord with the observation results by the DARTs in Figure 2. In addition, the direction slightly turns around counterclockwise, suggesting that the horizontal velocities on the western area close to the Kuril and Japan trenches are larger than that on the eastern area. As shown in the bottom right panel of Figure 3, the TIDs propagate to the epicenter at about 12:20 UT.

The time-distance map of vTEC variations is usually used to estimate the velocity of disturbances with a point origin, such as the epicenter. However, the origin for the reflected tsunami is not a point but a line (the Emperor seamounts). So, the method obtaining the velocity of disturbances by time-distance map is not suitable. Here, we estimate the horizontal velocities of the TIDs in vTEC variations following the approach of Garrison et al. (2007). The horizontal velocities of the TIDs vary 240-290 m/s approximately from eastern area to western area, which is consistent to the observed results in the ionospheric maps. According to the ocean depths (h) from ETOPO1 grid data supplied by U.S. NOAA (about 5900-9000 m at adjacent area), the tsunami velocities are about 242-300 m/s obtained from the shallow-water equation $v=\sqrt{gh}$ with gravity (g) of 9.8 m/s^2. This indicates the horizontal velocities of the observed TIDs are similar to the tsunami velocities at the sea-level.

To further examine the correlation of TIDs and tsunami waves, we plot vTEC variation time-series derived from satellite PRN 25 and satellite PRN 29 in Figure 4 (The TIDs are observed by the two satellites). Compared Figure 4 and Figure 2, it is easy to find the waveform of the TIDs is very similar to that of the reflected tsunami waves at the sea-level. According to the time-frequency diagrams, the center frequency of the TIDs is about 0.55 mHz, which is larger than that of the reflected tsunami waves. This can be attributed to the Doppler Effect caused by the relative motion between the GPS satellite and the TIDs. As seen from Figure 1, the direction of PRN 25 or PRN 29 is almost opposite to the TIDs, leading to the shortened period when observe the disturbances. The center frequency of TIDs is about 0.44 mHz after amending the Doppler Effect, which is basically consistent to that of reflected tsunami waves.

According to the NOAA's MOST model for this event, the direction of the reflected tsunami waves at the sea-level is also southwest and turns around counterclockwise, which is consistent to that of the observed TIDs in Figure 3. As described in the previous section, the reflected tsunami waves reach the epicenter at about 6 h after the earthquake. So, the observed time for the TIDs and reflected tsunami is basically consistent with ~35 min delay. The magnitude of the observed delay is also observed on the case of 2009 Samoa tsunami (Rolland et al., 2010), which might be due to combined influence of thin shell approximation, horizontal wind and horizontal delay when IGWs propagated to the ionosphere. The horizontal group velocity of IGWs at different height is always smaller than the tsunami velocity, leading to the horizontal delay when propagating to the ionosphere (Occhipinti et al., 2013). According to the HWM93 wind model (Hedin et al, 1991), the background horizontal winds propagate along the northwest at the studied times and areas, which are opposite to that of tsunami waves. When IGWs propagate against the winds, the horizontal group velocity will decrease (Ding et al., 2003), further prolonging the horizontal delay.

According to above analysis, the observed TIDs have similar horizontal velocity, direction, period, waveform and observed time compared to the reflected tsunami waves at the sea-level. Furthermore, to remove possible recurrent TIDs, we also verified that there weren't significant perturbations on the day before and after the event day at the study times. These results can confirm that the observed TIDs in Figure 3 are triggered by the reflected tsunami waves. This is the first time that the reflected tsunami signature in ionosphere is detected by the GPS TEC.

4 Conclusions

In this paper, we firstly analyze the tsunami measurements recorded by two DART buoys provided by the NDBC of U.S. NOAA after the 11 March 2011 earthquake, demonstrating that the straight tsunami waves from mainshock are reflected when propagating to the underwater obstacles. Then, we employ the two-dimensional maps of vTEC variations extracted from very dense Japanese GEONET GPS data to observe disturbances in ionosphere. The observed TIDs have similar propagation characteristics in terms of horizontal velocity, direction, waveform, period and observation time compared to the reflected tsunami waves at the sea-level, suggesting the TIDs are triggered by the reflected tsunami waves. The observed results in this study confirm the IGWs generated by reflect tsunami can also propagate upward to the atmosphere and interact with the plasma at the ionospheric height.

The results indicate not only the straight tsunami from mainshock, but also the reflected tsunami might have potential to induce ionospheric disturbances. This study provides a new recognition of tsunami-driven TIDs and support for the future tsunami warning system.

Acknowledgments

The GPS data used in this study are provided by the GeoSpatial Information authority (GSI) of Japan (ftp: //terras.gsi.go.jp). The DART data are provided by the National Data Buoy Center (NDBC) of U.S. National Oceanic and Atmospheric Administration (NOAA). This study was supported by National Natural Science Foundation of China (Grant No. 41231064, 41204028) and the Surveying and Mapping Foundation Research Fund Program, National Administration of Surveying, Mapping and Geoinformation (13-02-07).

References

Artru, J., Ducic, V., Kanamori, H., Lognonné, P., and Murakami, M.: Ionospheric detection of gravity waves induced by tsunamis, Geophys J Int, 160, 840-848, 2005.

DasGupta, A., Das, A., Hui, D., Bandyopadhyay, K. K., and Sivaraman, M. R.: Ionospheric perturbations observed by the GPS following the December 26th, 2004 Sumatra-Andaman earthquake, Earth Planets Space, 58, 167, 2006.

Ding, F., Wan, W., and Yuan, H.: The influence of background winds and attenuation on the propagation of atmospheric gravity waves, J Atmos Sol-Terr Phy, 65, 857-869, 2003.

Galvan, D. A., Komjathy, A., Hickey, M. P., and Mannucci, A. J.: The 2009 Samoa and 2010 Chile tsunamis as observed in the ionosphere using GPS total electron content, Journal of Geophysical Research: Space Physics (1978–2012), 116, 2011.

Garrison, J. L., Lee, S. C. G., Haase, J. S., and Calais, E.: A method for detecting ionospheric disturbances and estimating their propagation speed and direction using a large GPS network, Radio Sci, 42, 2007.

Hedin, A. E., Biondi, M. A., Burnside, R. G., Hernandez, G., Johnson, R. M., Killeen, T. L., Mazaudier, C., Meriwether, J. W., Salah, J. E., and Sica, R. J.: Revised global model of thermosphere winds using satellite and ground‐based observations, Journal of Geophysical Research: Space Physics (1978–2012), 96, 7657-7688, 1991.

Hernández-Pajares, M., Juan, J. M., and Sanz, J.: Medium‐scale traveling ionospheric disturbances affecting GPS measurements: Spatial and temporal analysis, Journal of Geophysical Research: Space Physics (1978–2012), 111, 2006.

Hickey, M. P., Schubert, G., and Walterscheid, R. L.: Propagation of tsunami‐driven gravity waves into the thermosphere and ionosphere, Journal of Geophysical Research: Space Physics (1978–2012), 114, 2009.

Hines, C. O.: Gravity waves in the atmosphere, Nature, 239, 73-78, 1972.

Liu, J. Y., Tsai, Y. B., Chen, S. W., Lee, C. P., Chen, Y. C., Yen, H. Y., Chang, W. Y., and Liu, C.: Giant ionospheric disturbances excited by the M9. 3 Sumatra earthquake of 26 December 2004, Geophys Res Lett, 33, 2006.

Nat. Hazards Earth Syst. Sci. Discuss., doi:10.5194/nhess-2016-11, 2016
Manuscript under review for journal Nat. Hazards Earth Syst. Sci.
Published: 26 January 2016

Natural Hazards and Earth System Sciences
Discussions

Liu, J. Y., Chen, C. H., Lin, C. H., Tsai, H. F., Chen, C. H., and Kamogawa, M.: Ionospheric disturbances triggered by the 11 March 2011 M9. 0 Tohoku earthquake, Journal of Geophysical Research: Space Physics (1978–2012), 116, 2011.

Mai, C. L., and Kiang, J. F.: Modeling of ionospheric perturbation by 2004 Sumatra tsunami, Radio Sci, 44, 2009.

Makela, J. J., Lognonné, P., Hébert, H., Gehrels, T., Rolland, L., Allgeyer, S., Kherani, A., Occhipinti, G., Astafyeva, E., and Coïsson, P.: Imaging and modeling the ionospheric airglow response over Hawaii to the tsunami generated by the Tohoku earthquake of 11 March 2011, Geophys Res Lett, 38, 2011.

Occhipinti, G., Lognonné, P., Kherani, E. A., and Hébert, H.: Three‐dimensional waveform modeling of ionospheric signature induced by the 2004 Sumatra tsunami, Geophys Res Lett, 33, 2006.

Occhipinti, G., Coisson, P., Makela, J. J., Allgeyer, S., Kherani, A., Hebert, H., and Lognonné, P.: Three-dimensional numerical modeling of tsunami-related internal gravity waves in the Hawaiian atmosphere, Earth, planets and space, 63, 847-851, 2011.

Occhipinti, G., Rolland, L., Lognonné, P., and Watada, S.: From Sumatra 2004 to Tohoku‐Oki 2011: The systematic GPS detection of the ionospheric signature induced by tsunamigenic earthquakes, Journal of Geophysical Research: Space Physics, 2013.

Occhipinti, G.: The seismology of the planet Mongo: The 2015 ionospheric seismology review, Subduction Dynamics: From Mantle Flow to Mega Disasters, 211, 169, 2015.

Peltier, W. R., and Hines, C. O.: On the possible detection of tsunamis by a monitoring of the ionosphere, Journal of Geophysical Research, 81, 1995-2000, 1976.

Rolland, L. M., Occhipinti, G., Lognonné, P., and Loevenbruck, A.: Ionospheric gravity waves detected offshore Hawaii after tsunamis, Geophys Res Lett, 37, 2010.

Rolland, L. M., Lognonné, P., Astafyeva, E., Kherani, E. A., Kobayashi, N., Mann, M., and Munekane, H.: The resonant response of the ionosphere imaged after the 2011 off the Pacific coast of Tohoku Earthquake, Earth, planets and space, 63, 853-857, 2011.

Rozhnoi, A., Shalimov, S., Solovieva, M., Levin, B., Shevchenko, G., Hayakawa, M., Hobara, Y., Walker, S. N., and Fedun, V.: Detection of tsunami‐driven phase and amplitude perturbations of subionospheric VLF signals following the 2010 Chile earthquake, Journal of Geophysical Research: Space Physics, 2014.

Tang, L., Titov, V. V., Wei, Y., Mofjeld, H. O., Spillane, M., Arcas, D., Bernard, E. N., Chamberlin, C., Gica, E., and Newman, J.: Tsunami forecast analysis for the May 2006 Tonga tsunami, Journal of Geophysical Research, 113, C12015, 2008.

Tang, L., and Zhang, X.: A Multi-Step Multi-Order Numerical Difference Method for Traveling Ionospheric Disturbances Detection. China Satellite Navigation Conference (CSNC) 2014 Proceedings: Volume II, Springer, 2014.

Tang, L., Zhang, X., and Li, Z.: Observation of ionospheric disturbances induced by the 2011 Tohoku tsunami using far-field GPS data in Hawaii, Earth, Planets and Space, 67, 1-7, 2015.

Tsugawa, T., Saito, A., Otsuka, Y., Nishioka, M., Maruyama, T., Kato, H., Nagatsuma, T., and Murata, K. T.: Ionospheric disturbances detected by GPS total electron content observation after the 2011 off the Pacific coast of Tohoku Earthquake, Earth, planets and space, 63, 875-879, 2011.

Zhang, X., and Tang, L.: Detection of ionospheric disturbances driven by the 2014 Chile tsunami using GPS total electron content in New Zealand, Journal of Geophysical Research: Space Physics, 120, 7918-7925, 2015.

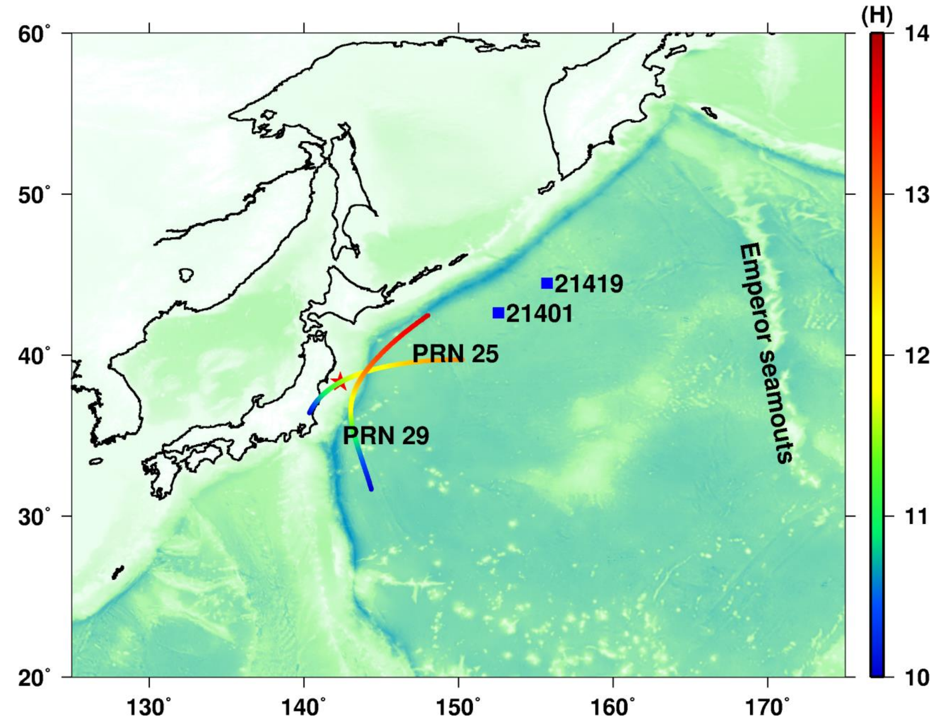

Figure 1. The locations of epicenter, DART stations and IPPs. The red pentagram indicate the epicenter of 2011 Tohoku earthquake, the blue squares note the DART stations and the color bar denotes the observation time of IPPs.

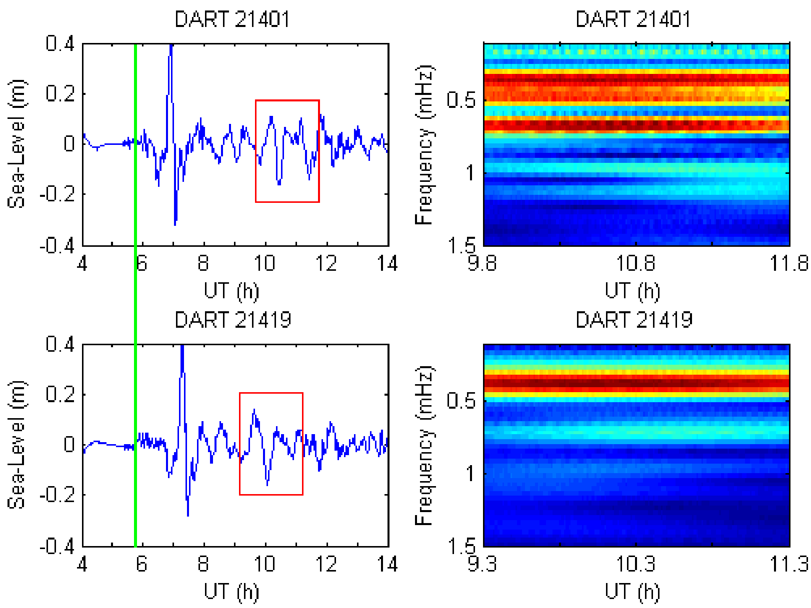

Figure 2. The sea-level tsunami series and time-frequency diagrams. The left panels are sea-level tsunami measurements recorded by the DART 21401 and DART 21419. The right panels are corresponding time-frequency diagrams for the time-series of the tsunami signals denoted by red rectangles. The green line in the left panels indicates the time of earthquake.

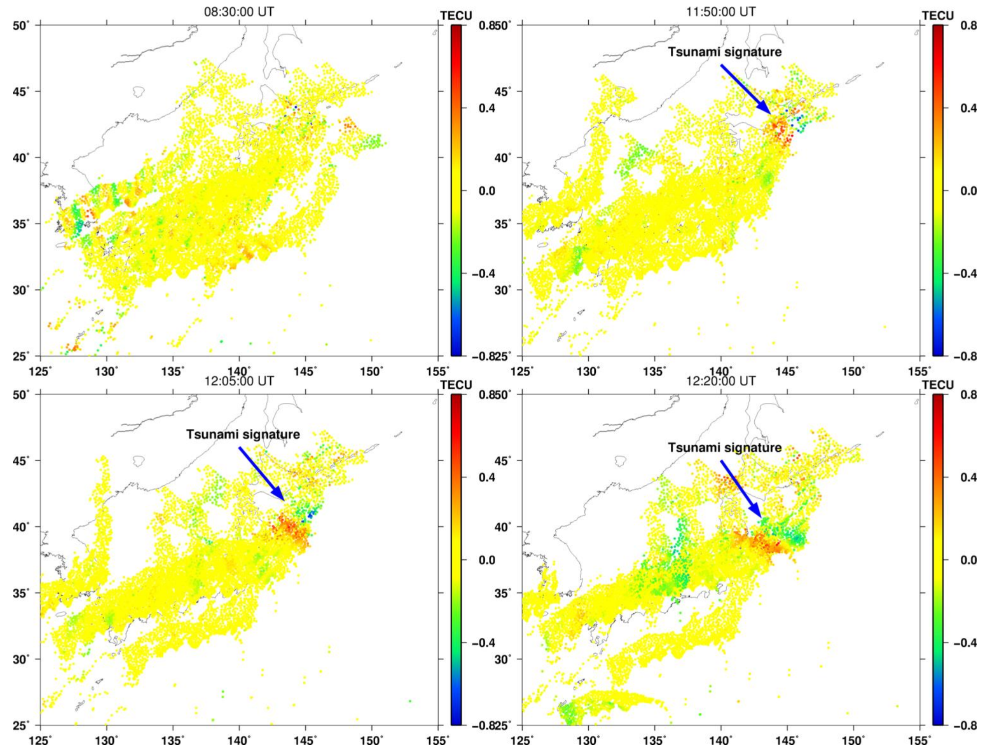

Figure 3. The two-dimensional maps of vTEC variations derived from GPS observations in GEONET. At about 08:30 UT, the ionospheric disturbances induced by origins from epicenter (Rayleigh wave, acoustic wave, etc.) are basically invisible. At about 11:50 UT, the ionospheric signature driven by reflected tsunami wave is appeared.

Nat. Hazards Earth Syst. Sci. Discuss., doi:10.5194/nhess-2016-11, 2016
Manuscript under review for journal Nat. Hazards Earth Syst. Sci.
Published: 26 January 2016

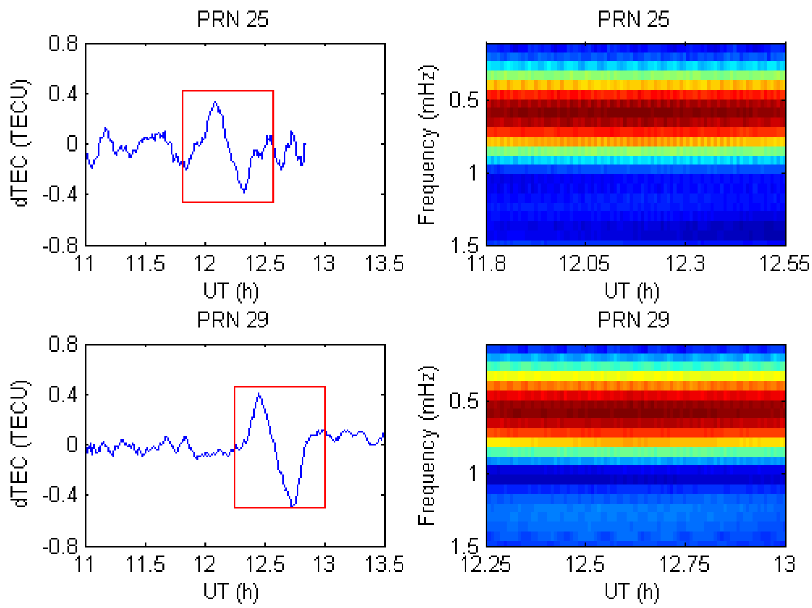

Figure 4. The vTEC variation series and time-frequency diagrams. The left panels are vTEC variation series derived from satellite PRN 25 and satellite PRN 29. The right panels are corresponding time-frequency diagrams for the time-series of the tsunami signals denoted by red rectangles.